Journal of Applied Chemistry JAC http://chemistry.journals.semnan.ac.ir

Mesoporous Titanium Dioxide Nanoparticles: Synthesis, Characterization and Application as Photocatalyst for Removing of Phenazopyridine

Azadeh Hajesmaili[a], Zohreh Bahrami[a*]

[a] *Faculty of Nanotechnology, Semnan University, Semnan, Iran*

Article history:
Received:6/Jun/2014
Received in revised form: 10/Jul/2014
Accepted: 25/Jul/2014

Abstract

The mesoporous titanium dioxide nanoparticles were successfully prepared via a sol–gel method using cetyltrimethyl ammonium bromide (CTAB) as a soft template. The obtained samples were characterized by powder X-ray diffraction (PXRD), scanning electron microscopy (SEM), N_2 adsorption/desorption analysis, FTIR and UV–visible spectroscopies. The obtained results reveal that the all samples have anatase phase, spherical morphology and the mean size value less than 50 nm. With increasing the molar ratio of CTAB/titanates up to 1:5, the particle size decreases and the specific surface area increases. The performance of the synthesized nano-photocatalysts was measured by photocatalytic removal of phenazopyridine using UV irradiation light by 15 W (UV–C) mercury lamp emitted around 254 nm. The findings confirm that the photocatalytic activity of TiO_2 nanoparticles strongly is depends on the physical properties such as size and specific surface area. When the particle size is about 28 nm, the highest photocatalytic activity is observed.

Keywords: Mesoporous titanium dioxide, Nanoparticles, Photocatalytic removal, Soft template, Phenazopyridine.

1. Introduction

The photocatalytic oxidation of organic pollutants in water, as an advanced oxidation process (AOPs), has been proved to be an effective technique for purification and remediation of polluted water [1-4]. Photocatalyst destroys the pollutants by decomposing or transforming into less harmful substances in the presence of UV or near-UV radiation and this process can be operated at atmospheric pressure and near or slightly higher than room temperature [5]. Titanium dioxide (TiO_2) has excellent performance as a photocatalyst under UV irradiation because its fascinating features such as low cost, environmental benignity, good chemical stability, excellent electronic and optical properties [6]. TiO_2 has wide band gap (3.2 eV for anatase form, 3.0 eV for rutile form and 3.13 eV for brookite form) that have excellent potentials for degradation of organic pollutants [7].

Some success in enhancing the efficiencies of photocatalysts have been achieved by methods such as using nano-sized and mesoporous structure instead of bulk materials. These strategies lead to increasing the absorbing and decomposing pollutant and finally enhancing the photocatalytic activity.

[*].**Corresponding Author:** *E-mail address: bahrami.zoh@semnan.ac.ir; Tel.: +(98)2331533507*

Mesoporous TiO_2 is an interesting material for photocatalytic applications due to its continuous particle framework, which may be beneficial, compared to separated individual nanoparticles. There are some reports about photocatalytic application of mesoporous titanium dioxide. I. Tamiolakis et al. studied photocatalytic activity of highly crystalline mesoporous TiO_2 particles [8]. Y. Feng et al. used mesoporous TiO_2 for photodecomposition of toluene [9]. The application of mesoporous anatase TiO_2 for photocatalytic hydrogen evolution was investigated by Z. Zhang et al. [10]. The reasons for the low number of studies made on mesoporous TiO_2 as a photocatalyst are likely related to the difficulties in making it as an ordered material.

Different methods were used for preparing mesoporous titanium dioxide such as hydrothermal [11], evaporation-induced self-assembly [12], ultrasonic irradiation [13], and sol–gel [14]. Recently, mesoporous TiO_2 have been well synthesized with use of organic surfactant templates. Templates were used as structure-directing agents for organizing network forming of TiO_2 and mixed oxide species in non-aqueous solutions.

Phenazopyridine ($C_{11}H_{11}N_5$) (Fig. 1) is used as analgesic drug in urinary tract treatment and other medical prescriptions. The presence of the azo group made it a stable compound. Phenazopyridine is potentially a carcinogenic material and it can cause serious effects on human health. Therefore, design of a suitable process for degradation of phenazopyridine from water is an important issue.

In this paper, we focused on the preparation of mesoporous titanium dioxide nanoparticles for removing of phenazopyridine from water. For this purpose, cetyl trimethyl ammonium bromide (CTAB) was used as a soft template via the sol-gel method. In fact, combination of the two methods, template synthesis and sol-gel was used for the preparation of mesoporous titanium dioxide nanoparticles.

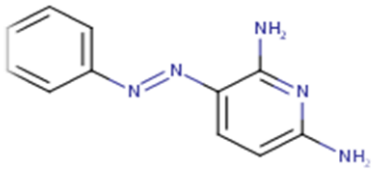

Figure 1. Chemical structure of phenazopyridine.

2. Experimental procedure

2.1 Materials and Methods

All chemicals were of analytical grade, obtained from commercial sources and used without further purification: absolute ethanol (99.99%), tetra-n-butyl orthotitanate ($C_{16}H_{36}O_4Ti$), cetyl trimethylammoniumbromide (CTAB), and phenazopyridine (M_w=213.239 g/mol) as a model drug contaminant.

The used characterization techniques are listed as below:

X-ray diffraction (XRD) was used to identify the structure and average crystallite size of the obtained photocatalysts. A PHILIPS-PW1800 XRD system generating monochromated Cu Kα radiation with operating conditions of 40 kV and 30 mA was used to obtain the XRD pattern. N_2 adsorption–desorption isotherms of the samples were obtained by using a nitrogen adsorption–desorption apparatus (PHS-1020(PHS CHINA) at a liquid nitrogen temperature -196 °C. Brunauer–Emmett–Teller (BET) approach using adsorption data over the relative pressure ranging from 0 to 0.8 was utilized to determine the specific surface areas of the photocatalyst. Barrett–Joyner–Halenda (BJH) method was used to determine the pore size distribution of the photocatalysts. UV–vis spectra were obtained by using a UV–vis spectrophotometer (Rayleigh UV-1600) at the wavelength of 430 nm. Morphology of the samples was investigated by using a scanning electron microscope (KYKY EM-3200) operated 200 kV. The FTIR spectra were recorded using Equinox 55 spectrometer in the range between 400 and 3400 cm^{-1}. UV–vis diffuse reflectance spectroscopy (UV-vis DRS) of sample was obtained using AvaSpec–2048 TEC spectrometer for determination of the optical

band gap (E_g). E_g was calculated by the following equation [15]:

$$E_g=hc/\lambda \quad (1)$$

Where Eg is the optical band gap energy (eV), h is the Plank's constant, c is the light speed (m s^{-1}), and λ is the wavelength (nm).

2.2 Synthesis of mesoporous titanium dioxide nanoparticles (M-TiO_2)

Tetra-n-butyl orthotitanate (TBOT) and cetyl trimethylammoniumbromide (CTAB) were used as titania source and soft template, respectively. The desired amount of CTAB was dissolved in a mixture of water and absolute ethanol in a volume ratio of 4/1 and stirred to form a clear solution. Calculated amount of tetra-n-butyl orthotitanate (CTAB/TBOT molar ratio 1:1, 1:3, 1:5 and 1:7) was added drop wise with continuous vigorous stirring to the obtained clear solution. The resulting gel was further stirred for 24 h and the precipitate was centrifuged and washed several times with distilled water. The final product was calcined at 450 ˚C for 6 h in static air to remove CTAB.

2.3 Photocatalysis experiment

Photocatalytic removal experiment was carried out at the room temperature in a batch quartz reactor. Artificial irradiation was provided by 15 W (UV–C) mercury lamp (Philips, Holland) emitted around 254 nm, which positioned on the top of the batch quartz reactor. 40 mg of mesoporous titania nanoparticles was dispersed in 100 mL water for 15 min using an ultrasonic bath (Elma T460/H, 35 kHz, 170 W), then desired amount of phenazopyridine solution (10 mg L^{-1}) was transferred into the reactor and was stirred for 30 min to achieve the adsorption equilibration in the dark before irradiation. The photocatalytic reaction was started by turning on the light source. At the given irradiation time, the sample (5 mL) was taken out, and phenazopyridine concentration controlled by UV–vis spectrophotometer at λ_{max} = 430 nm.

3. Results and discussion

3.1 PXRD analysis

The crystal structure and crystallite size of the synthesized M-TiO_2 nanoparticles at different CTAB/TBOT molar ratio, were identified by X-ray diffraction (XRD) patterns (Fig. 2). As it could be observed, the all samples have same pattern and increasing the CTAB/TBOT molar ratio don't change the crystal structure. The intense and sharp peaks elucidated that the nanoparticles are well crystallized and have anatase structure (JPCDS card: 01-073-1764). The observed peaks at around 25°, 38°, 48°, 54°, 55°, 62°, 69°, 70° and 75.5° can be assigned to the reflections of (101), (112), (200), (105), (211), (204), (116), (220) and (215) crystal planes, respectively.

The crystallite size of mesoprous titania was estimated from line broadening of the (101) diffraction peak using Scherrer's equation:

$$D = \frac{K\lambda}{\beta\cos\theta} \quad (2)$$

Where D is the average crystallite size (nm), λ is the wavelength of the X-ray radiation, K is a constant taken as 0.89, β is the full width at half maximum intensity, and θ is the half diffraction angle.

The crystallite size was found to be in the range of 18–42 nm (Table1).

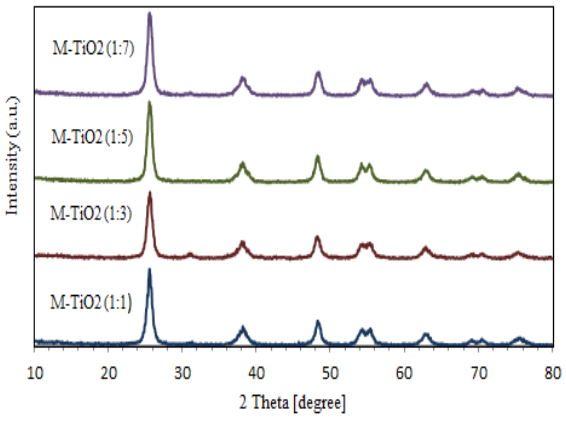

Figure 2. XRD patterns of the synthesized M-TiO_2 nanoparticles at different CTAB/TBOT molar ratio.

3.2 Morphology analysis

In order to understand the morphological features of the template synthesized M-TiO_2 nanoparticles, calcined powders were analyzed using FESEM. Fig. 3 shows the scanning electron micrographs of the all samples. As represented in Fig.3, the morphology of the nanoparticles is spherical and the mean size value is less than 50 nm. Except of M-TiO_2 (1:7) sample, with increasing the molar ratio of CTAB/TBOT, the size of nanoparticles decreases. These finding are in agreement with XRD data and can be explained by the mechanism of the formation of these mesoporous TiO_2 nanoparticles.

Two mechanisms have been proposed to interpret the formation of mesoporous materials by template method. One is liquid crystal mechanism [16], and another is co-operative mechanism [17], which has been proposed for the formation of mesoporous materials at high and low surfactant concentration, respectively. In the present experiment, the concentration of surfactant being low (0.01M), and we consider the co-operative mechanism to understand for the formation of mesoporous titania nanoparticles. The surfactant molecules used in the present study consists of a polar head and hydrocarbon chain that in an aqueous media, are forming normal micelles. At low surfactant concentration the normal micelle is spherical, with a diameter fixed by the length of the hydrocarbon chain and the size of the polar head. The formation of the mesoporous titania begins with hydrolysis and condensation of the titanate source on the surface of micelles formed by surfactant self-assembly in aqueous solution.

The hydrolysis and condensation of titanate happens simultaneously. Since the hydrolyzed titanate monomers are negatively charged, they are adsorbed onto positively charged CTAB micelles electrostatically and after condensation, a titanate shell is formed around a micelle. With increasing the concentration of TBOT up to molar ratio 1:5, the all micelles will have titanate shell around themselves. In this case, micelles are separated from each other and the smaller particles are formed. When the concentration of TBOT reached to molar ratio = 1:7, the neighbouring micelles with a titanate shell start to aggregate, which produces the nuclei for the particle growth. With the growth of nuclei and continuous hydrolysis and condensation, larger particles are obtained [18]. Therefore, as it could be observed in SEM images, the M-TiO_2 (1:7) sample is mixture of nanoparticles and bulk mesoporous material. These results reveal that the molar ratio 1:7 of CTAB/TBOT, can not be appropriate to synthesize the M-TiO_2 nanoparticles.

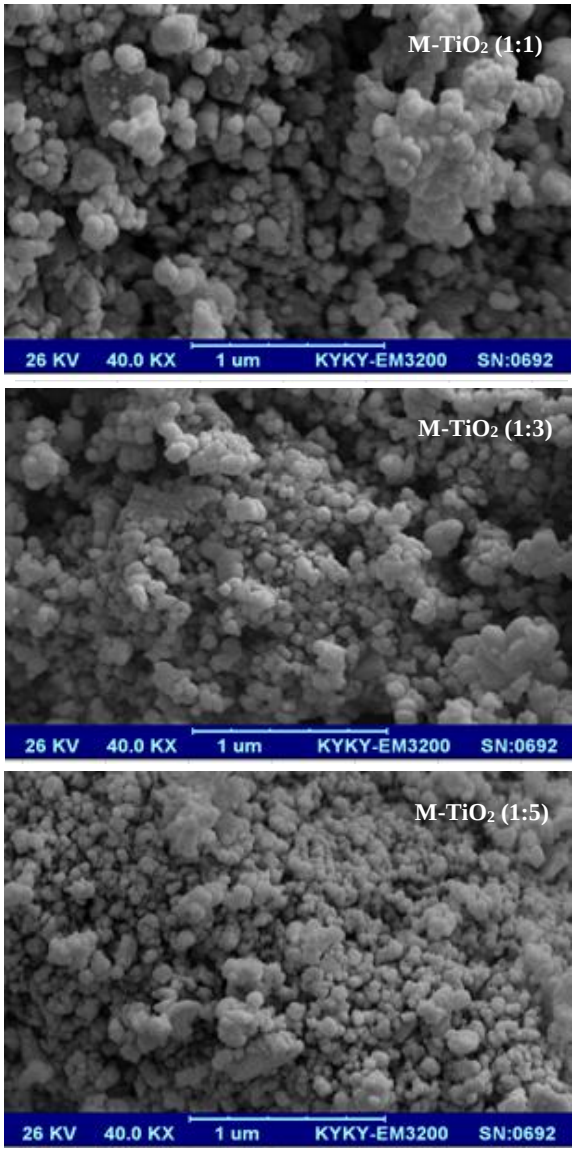

Figure 3. SEM images of the M-TiO_2 nanoparticles.

3.3 N_2 adsorption/desorption measurement

Textural characterization of the samples was made by N_2 adsorption/desorption and the obtained results are

presented in Fig.4 and Table 1. The isotherms reveal a typical type IV pattern (according to IUPAC classification) with a hysteresis loop ($0.4 < P/P_o < 0.8$), that is a typical characteristic of mesoporous materials. The BJH pore size distribution obtained from the adsorption branch of the isotherms appears to be narrow (Fig. 4b).

With increasing the molar ratio of CTAB/TBOT up to 1:5, surface area increases and reaches to 93 $m^2.g^{-1}$ that is about two times higher than that of P25 powder (50 $m^2.g^{-1}$). By more increasing of the molar ratio, the surface area decreases. The highest pore size is related to M-TiO_2 (1:3) sample that equal to 7 nm. The results of nitrogen adsorption/desorption experiments indicate that the titanium dioxide nanoparticles prepared by this soft-template method have large specific surface area with mesoporous structure.

Table.1: Pore size (d_p) , pore volume (V_p), specific surface area (a_s), and average crystallite size of M-TiO_2 synthesized at different CTAB/TBOT molar ratio.

CTAB/TBOT	d_p (nm)	V_p (cm^3/g)	a_s (m^2/g)	crystallite size (nm)
1:1	5.42	0.135	69.85	32.93
1:3	7.00	0.210	83.76	28.21
1:5	6.40	0.257	93.05	18.41
1:7	5.42	0.157	70.36	41.37

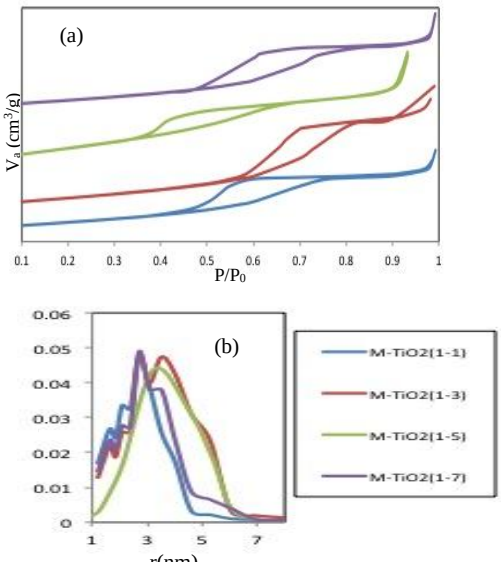

Figure 4. (a) N_2 adsorption/desorption isotherms and (b) BJH pore size distribution of the M-TiO_2 nanoparticles.

3.4 FTIR analysis

FTIR spectra of the all synthesized samples were measured in the range of 400-3400 cm^{-1} and illustrated in Fig. 5. For the all samples, the strong peak around 500 cm^{-1} attributed to Ti-O-Ti lattice vibrations, which indicates their crystalline structure [19]. The weak peaks at about 1640 cm^{-1} correspond to O–H groups and show the presence of water of hydration in the samples [20].

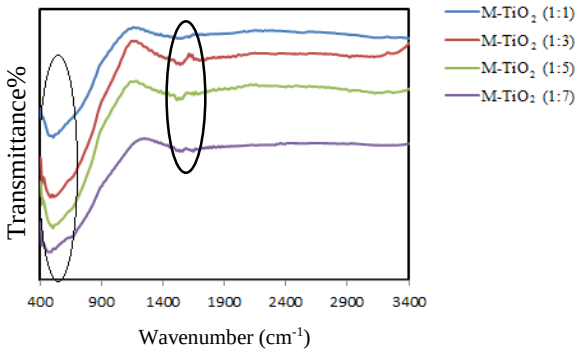

Figure 5. FTIR spectra of the all synthesized samples.

3.5 UV-vis DRS analysis

The Optical properties of the samples were studied by UV-vis diffuse reflectance spectroscopy (DRS). Fig. 6 shows the UV-vis DRS spectra of the all samples. The maximum absorbance of M-TiO_2(1:1), M-TiO_2(1:3), M-TiO_2(1:5) and M-TiO_2(1:7) is observed at 408, 405, 405 and 406 nm, respectively. The Eg value calculated from the Eq. (1) is 3.04, 3.06, 3.06 and 3.05 eV that related to the samples with different molar ratio (1:1, 1:3, 1:5 and 1:7) of CTAB/TBOT, respectively.

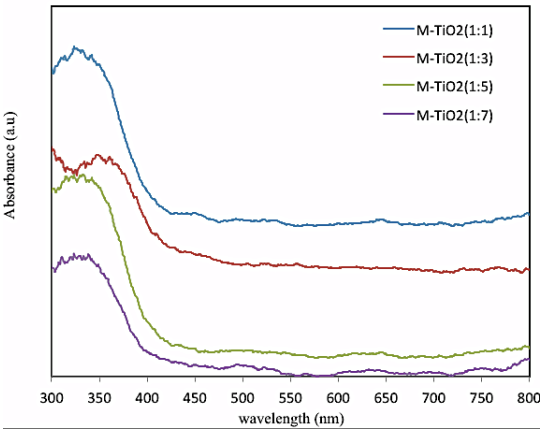

Figure 6. The UV-vis DRS spectra of the M-TiO_2 nanoparticles.

3.6 Photocatalytic study

The photocatalytic activity of the M-TiO_2 nanoparticles was determined by the degradation of phenazopyridine under UV light irradiation. The photocatalytic degradation rate (DR%) was calculated by the following formula [21]:

$$DR\% = [1-(C/C_0)]*100\% = [1-(A/A_0)]*100\% \quad (3)$$

Where, C_0 is the initial concentration of phenazopyridine before degradation, C is the concentration at the certain reaction time, A_0 is the UV–vis absorption of the original solution and A is the UV–vis absorption of degraded solution at the certain time.

Fig.7 represents the photodegradation curves of phenazopyridine without photocatalyst and by M-TiO_2 nanoparticles. As it could be seen, DR% of phenazopyridine without photocatalyst is reached to 5% after 90 min irradiation. The maximum and minimum DR% is related to the M-TiO2(1:3) and M-TiO2(1:1) samples, respectively. The obtained results reveal that the photocatalytic activity of TiO_2 nanoparticles strongly is depends on the physical properties such as size and specific surface area. When the particle size is about 28 nm, the highest photocatalytic activity is observed.

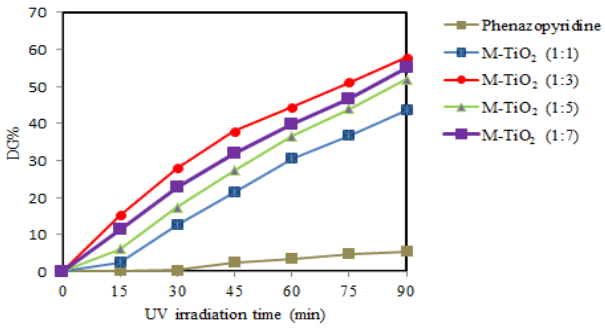

Figure 7. Photodgradation curves of phenazopyridine without photocatalyst and by M-TiO_2 nanoparticles.

4. Conclusion

Mesoporous TiO_2 nanoparticles with different CTAB/TBOT molar ratio were successfully prepared via a sol–gel method. The obtained results indicated that the all M-TiO_2 samples have pure anatase phase and spherical morphology. With increasing the molar ratio of CTAB/TBOT, the particle size decreases and the specific surface area increases. The photocatalytic performance of the prepared M-TiO_2 was studied toward removal of phenazopyridine under UV irradiation. The maximum photocatalytic activity is observed when the particle size is about 28 nm. In addition, mesoporous structure provides an appreciable surface area, thereby facilitating the photodegradation of the phenazopyridine. These findings confirm that the synthesized M-TiO_2 nanoparticles have good photocatalytic activity.

Acknowledgments

The authors would appreciate Semnan University for financial support.

References

[1] A. A. Ismail, D. W. Bahnemann, *J. Mater. Chem.* **21** (2011) 11686.

[2] B. Khodadadi, *J. Appl. Chem.* **8** (2013) 61.

[3] L. Zaman, *J. Appl. Chem.* **10** (2015) 107.

[4] M. M. Momeni, *J. Appl. Chem.* **11** (2016) 121.

[5] P. Jantawasu, T. Sreethawonga, S. Chavadej, *Chem. Eng. J.* **155** (2009) 223.

[6] E. Masolo , M. Meloni , S. Garroni , G. Mulas , S. Enzo , M. D. Baró , E. Rossinyol , A. Rzeszutek , I. H.Geppert, M. Pilo, *Nanomaterials.* **4** (2014) 583.

[7] T. Sreethawong, Y. Suzuki, S.Yoshikawa, *J. Solid State Chem.* **178** (2005) 329.

[8] B. K. Mutuma, G. N. Shao, W. D. Kim, H. T. Kim , *J. Colloid Interface Sci.* **442** (2015) 1.

[9] S. Pavasupree, J. Jitputti, S. Ngamsinlapasathian, S. Yoshikawa, *Mater. Res. Bull.* **43** (2008) 149.

[10] I. M. Hung, Y. Wang, C. Fa Huang, Y. S. Fan, Y. J. Han, H. W. Peng, *J. Euro. Ceramic Soc.* **30** (2010) 2065.

[11]. M. Zhou, J. Yu, B. Cheng, *J. Hazard. Mater. B* **137** (2006) 1838.

[12] B. Palanisamy, C.M. Babu, B. Sundaravel, S. Anandan, V. Murugesan, *J. Hazard. Mater.* **252– 253** (2013) 233.

[13] K. Zhang, X. Wang, X. Guo, T. He, Y. Feng, *J. Nanopart. Res.***16** (2014) 2246.

[14] L. L. Costa, A. G. S. Prado, *Photochem. Photobio. A: Chem.* **201** (2009) 45.

[15] I. Tamiolakis, I. N. Lykakis, A. P. Katsoulidis, G.S. Armatas, *Chem. Commun.* **48** (2012) 6687.

[16] S. De, S. Dutta, A. K. Patra, A. Bhaumik, B. Saha, *J. Mater. Chem.* **21** (2011) 17505.

[17] Y. Y. Feng, L. Li, M Ge, C. Guo, J. Wang, Lu Liu, *Appl. Mater. Interfaces*, **2** (2010) 3134.

[18] Z. Yi, L. F. Dumee, C. J. Garvey, *Langmuir*, **31** (2015) 8478.

[19] S. Chu, L. Lou, *Appl. Surf. Sci.* **258** (2012) 9664.

[20] A. Sun, Z. Li, *Powder Tech.* **201** (2010) 130.

[21] Z. Zhang, F. Zuo, P. Feng, *Mater. Chem. Phys.* **20** (2010) 2206.